

Urine Metabolite Profiles Predictive of Human Kidney Allograft Status

Karsten Suhre,^{*†} Joseph E. Schwartz,^{‡§} Vijay K. Sharma,[§] Qiuying Chen,^{||} John R. Lee,[§] Thangamani Muthukumar,[§] Darshana M. Dadhania,[§] Ruchuang Ding,[§] David N. Ikle,[¶] Nancy D. Bridges,^{**} Nikki M. Williams,^{**} Gabi Kastenmüller,[†] Edward D. Karoly,^{††} Robert P. Mohny,^{††} Michael Abecassis,^{‡‡} John Friedewald,^{§§} Stuart J. Knechtle,^{|||} Yolanda T. Becker,^{|||} Benjamin Samstein,^{¶¶} Abraham Shaked,^{***} Steven S. Gross,^{||} and Manikkam Suthanthiran[§]

*Department of Physiology and Biophysics, Weill Cornell Medical College in Qatar, Doha, Qatar; †Institute of Bioinformatics and Systems Biology, Helmholtz Zentrum München, German Research Center for Environmental Health, Neuherberg, Germany; ‡Department of Psychiatry, Stony Brook University, Stony Brook, New York; §Division of Nephrology and Hypertension, Departments of Medicine and Transplantation Medicine, New York Presbyterian Hospital—Weill Cornell Medical Center, New York, New York; ¶Department of Pharmacology, Weill Cornell College of Medicine, New York, New York; ¶Rho Federal Systems, Chapel Hill, North Carolina; **National Institute of Allergy and Infectious Diseases, Bethesda, Maryland; ††Metabolon, Inc., Durham, North Carolina; ‡‡Division of Surgery—Organ Transplantation, Northwestern University Feinberg School of Medicine, Chicago, Illinois; §§Division of Nephrology—Organ Transplantation, Northwestern University Feinberg School of Medicine, Chicago, Illinois; |||Division of Surgery, Department of Surgery, University of Wisconsin Hospitals and Clinics, Madison, Wisconsin; ¶¶Division of Transplantation, Department of Surgery, Columbia University College of Physicians and Surgeons, New York, New York; and ***Department of Surgery, University of Pennsylvania School of Medicine, Philadelphia, Pennsylvania

ABSTRACT

Noninvasive diagnosis and prognostication of acute cellular rejection in the kidney allograft may help realize the full benefits of kidney transplantation. To investigate whether urine metabolites predict kidney allograft status, we determined levels of 749 metabolites in 1516 urine samples from 241 kidney graft recipients enrolled in the prospective multicenter Clinical Trials in Organ Transplantation-04 study. A metabolite signature of the ratio of 3-sialyllactose to xanthosine in biopsy specimen-matched urine supernatants best discriminated acute cellular rejection biopsy specimens from specimens without rejection. For clinical application, we developed a high-throughput mass spectrometry-based assay that enabled absolute and rapid quantification of the 3-sialyllactose-to-xanthosine ratio in urine samples. A composite signature of ratios of 3-sialyllactose to xanthosine and quinolate to X-16397 and our previously reported urinary cell mRNA signature of 18S ribosomal RNA, CD3ε mRNA, and interferon-inducible protein-10 mRNA outperformed the metabolite signatures and the mRNA signature. The area under the receiver operating characteristics curve for the composite metabolite–mRNA signature was 0.93, and the signature was diagnostic of acute cellular rejection with a specificity of 84% and a sensitivity of 90%. The composite signature, developed using solely biopsy specimen-matched urine samples, predicted future acute cellular rejection when applied to pristine samples taken days to weeks before biopsy. We conclude that metabolite profiling of urine offers a noninvasive means of diagnosing and prognosticating acute cellular rejection in the human kidney allograft, and that the combined metabolite and mRNA signature is diagnostic and prognostic of acute cellular rejection with very high accuracy.

J Am Soc Nephrol 27: 626–636, 2016. doi: 10.1681/ASN.2015010107

Received January 29, 2015. Accepted April 15, 2015.

Published online ahead of print. Publication date available at www.jasn.org.

Medical College, Division of Nephrology and Hypertension, Department of Medicine, 525 E. 68th Street, Box 3, New York, NY 10065. Email: msuthan@med.cornell.edu

Correspondence: Dr. Manikkam Suthanthiran, Weill Cornell

Copyright © 2016 by the American Society of Nephrology

Kidney transplantation is the preferred treatment for patients with end stage renal disease, but acute rejection, a frequent and serious post-transplant complication, undermines realization of the full benefits of this intervention. The invasive allograft biopsy performed to diagnose acute rejection has become safer over the years, but bleeding and graft loss still occur following a biopsy. Sampling errors and inter-observer variability in biopsy readings pose challenges and the feasibility and cost of repeated biopsies needed to capture anti-allograft immunity are major drawbacks. Development of noninvasive biomarkers of acute rejection is therefore a major objective of the field.

The multicenter, NIH-sponsored Clinical Trials in Organ Transplantation-04 (CTOT-04) investigated whether mRNA levels in urinary cells collected at the time of biopsy are diagnostic of acute rejection and whether mRNA profiles of sequential urine specimens obtained at clinically stable time points predict the future development of acute rejection.¹ Data from the CTOT-04 study demonstrated that a 3-gene signature of 18S rRNA and 18S-normalized CD3 ϵ mRNA and IP-10 mRNA (mRNA signature) in urinary cells discriminated acute cellular rejection (ACR) biopsies from biopsies without features of rejection (No Rejection biopsies). Furthermore, there was a sharp and significant rise in the diagnostic signature score during the weeks prior to an ACR biopsy.¹ However, despite the progress toward noninvasive characterization of kidney allograft status by mRNA profiling of urine from kidney graft recipients,^{1,2} there remains huge potential for further progress by probing the small molecule composition of these urines for ascertaining kidney allograft status.³

Metabolomics aims to measure all relevant small molecules (metabolites),³⁻⁸ and nontargeted metabolite profiling allows for the relative quantification of hundreds of metabolites in small volumes of biologic specimens such as urine. As both intermediate and end point markers of diverse biologic processes in the human body, observations of altered metabolite concentrations provide access to functionally relevant read-outs of perturbed disease-associated pathways in human metabolism.⁹⁻¹²

In this investigation, we used cell-free urine supernatants collected from the kidney transplant recipients enrolled in the CTOT-04 study to conduct a large-scale study of the urine metabolome to investigate whether urine metabolite profiles are diagnostic and prognostic of ACR. We further examined the diagnostic and prognostic performance of a combination of metabolites and the previously identified urinary cell mRNA signature. Finally, we developed a targeted high-throughput metabolomics assay for measurement of the identified metabolite signature in the clinical setting.

RESULTS

Urine Samples for Metabolomics

From a total of 4300 urine samples prospectively collected from the 485 kidney graft recipients (patients) enrolled in the parent CTOT-04 study, we selected 1518 urine samples from 242

patients for metabolomics (Figure 1) to include: (1) all 298 urine samples matched to 298 kidney allograft biopsies (urine samples collected from 3 days before to 1 day after the biopsy); (2) all 808 sequential urine samples preceding a biopsy diagnosis; and (3) all 412 urine samples from clinically stable patients who provided >10 sequential samples in the first 400 days of transplantation. We obtained high-quality data for 1516 urine samples from 241 kidney allograft recipients after exclusion of one patient and two samples (see Supplemental Material for details) regarding 749 different metabolites from 65 metabolic pathways, including 368 metabolites of unknown identity (Supplemental Table 1).

Urine Metabolites and ACR

Metabolite data from 50 urine samples matched to 50 ACR biopsies from 36 patients and 198 urine samples matched to 198 No Rejection biopsies from 149 patients were analyzed to determine whether metabolite profiles distinguish ACR biopsies from No Rejection biopsies.

Supplemental Table 2 lists the characteristics of transplant recipients, such as age, gender, ethnicity, race, and BMI. Among the 50 ACR biopsies graded using the Banff schema, 23 were graded as ACR grade IA, 11 as ACR grade IB, 12 as ACR grade IIA, 3 as ACR grade IIB and 1 as ACR grade III. The 198 biopsies classified as No Rejection biopsies did not show histologic features of ACR, AMR, borderline, bacterial infection/pyelonephritis, cytomegalovirus, polyomavirus type BK/polyoma nephropathy or post-transplant lymphoproliferative disease. However, several of the No Rejection biopsies displayed histologic changes consistent with ATN ($n=79$), tubular atrophy ($n=75$), interstitial fibrosis ($n=67$), glomerulosclerosis ($n=30$), vascular narrowing ($n=20$), calcineurin inhibitor toxicity ($n=18$), and/or recurrent disease ($n=2$). Also, several of the biopsies showed more than one histologic abnormality such as the presence of both interstitial fibrosis and tubular atrophy.

Kidney allograft function, measured at the time of biopsy, showed that the graft function was significantly inferior in the ACR biopsy group compared with the No Rejection biopsy group. As summarized in Supplemental Table 2, the mean (\pm SD) serum creatinine level at the time of kidney allograft biopsy in the ACR biopsy group was 3.7 ± 2.9 mg/dl (number of measurements = 37) and was 2.5 ± 2.3 mg/dl (number of measurements = 146) in the No Rejection biopsy group (Mann-Whitney $P < 0.001$), and the mean (\pm SD) estimated glomerular filtration rate (eGFR) in the ACR biopsy group was 30 ± 17 ml/min per 1.73 m^2 (number of measurements=37) compared with 43 ± 23 ml/min per 1.73 m^2 (number of measurements=146) in the No Rejection biopsy group (Mann-Whitney $P = 0.003$).

We also analyzed metabolite data from urine samples matched to antibody-mediated rejection, borderline changes, polyomavirus type BK nephropathy or other biopsy findings. Due to the small group sizes and the resulting lack of statistical power, results from these analyses are not included in this report.

Table 1 lists all metabolites and ratios of metabolites in urine that distinguished ACR biopsies from No Rejection

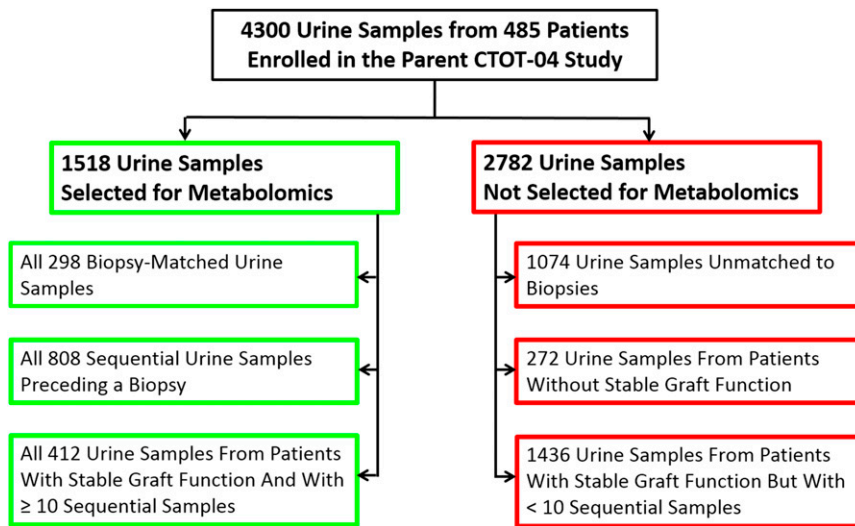


Figure 1. Selection of urine samples for metabolomics. From a total of 4300 urine samples prospectively collected from the 485 kidney allograft recipients (patients) enrolled in the parent CTOT-04 study, 1518 urine samples were selected for metabolite analysis to include the following urine samples: (1) all biopsy-matched urine samples, 298 samples matched to 298 kidney allograft biopsies performed in 190 patients (urine samples collected from 3 days before to 1 day after the biopsy); (2) all 808 sequential samples from 112 patients that preceded a first biopsy classified using Banff classification schema as acute cellular rejection, antibody-mediated rejection, borderline changes, or other, and sequential samples that preceded No Rejection biopsies; and (3) all 412 sequential samples from 40 patients with stable graft function and who had at least 10 sequential samples collected in the first 400 days of transplantation and with sufficient RNA for urinary cell mRNA profiling. The kidney allograft recipients designated as patients with stable graft function did not undergo biopsy during the 400 days of transplantation and met the following additional criteria: (1) average serum creatinine ≤ 2.0 mg/dl [$180 \mu\text{mol/l}$] at 6, 9, and 12 months following transplantation, (2) no treatment for acute rejection, and (3) no evidence of cytomegalovirus or polyomavirus type BK infection. Among the 1518 urine samples selected for metabolomics, one biopsy-matched urine sample from a patient with a No Rejection biopsy result was excluded from further analysis because of failed osmolality measurements, and one nonbiopsy-associated sample from a patient with other biopsy findings did not contain sufficient cell-free supernatant for nontargeted metabolite analysis. After exclusion of these two samples, high-quality metabolite data from 1516 samples collected from 241 kidney patients were available for data analysis. The number of patients in the three categories listed under the metabolomics exceeds 241 unique patients because several patients had multiple urine samples and contributed urine samples to more than one category, *i.e.*, the same patient contributing biopsy-matched urine sample as well as sequential urine samples and thereby counted in each category. A total of 2782 urine samples collected during the parent CTOT-04 study were excluded from nontargeted metabolite analysis because: (1) the urine samples were not matched to biopsy specimens or were collected following a biopsy (1074 specimens from 187 patients), (2) had unstable allograft function and no biopsy or were lost to follow-up (272 urine samples from 63 patients), or (3) had stable graft function but had less than 10 sequential samples collected in the first 400 days of transplantation; urine samples collected after 400 days and with insufficient RNA for mRNA profiling are also included in this group of 1436 specimens from 180 patients. The number of patients in the three categories excluded from metabolomics exceeds 243 unique patients because several patients had multiple urine samples and contributed urine samples to more than one category and thereby counted in each category. The colored boxes denote urine samples included for (green box) or excluded from (red box) urine metabolomics analysis.

biopsies at a false discovery rate of 5%.¹³ Supplemental Tables 3 and 4 provide all nominally significant associations (*i.e.*, with no adjustment for the number of tests) by linear regression (Supplemental Table 3) or logistic regression (Supplemental Table 4).

The ratio of the concentrations of the metabolites 3-sialyllactose to xanthosine (3SL/X) in the urine supernatant was strongly associated with ACR ($P=5.0 \times 10^{-8}$) and this ratio had the highest increase in the strength of association ($P\text{-gain}=2.0 \times 10^5$, compared with the association of the single metabolites in the ratio; for a definition of the $P\text{-gain}$ statistic see Methods and Petersen *et al.*¹⁴). The 3SL/X ratio was statistically significant even under conservative Bonferroni correction of the P value and the $P\text{-gain}$.

The diagnostic signature of the ratio of 3SL/X was not associated with age ($P=0.95$, Spearman rank-order correlation), gender ($P=0.52$, Mann–Whitney test), or ethnicity ($P=0.19$, Kruskal–Wallis analysis of variance). The signature was only weakly associated with eGFR ($P=0.054$, Spearman rank-order correlation, $r_s=-0.168$) and the 3SL/X ratio continued to be diagnostic of ACR after adjusting for eGFR.

A Composite Metabolite Signature of ACR

The ratio of 3SL/X showed by far the strongest $P\text{-gain}$ and was therefore considered the prime candidate for a metabolite signature. After controlling for the 3SL/X ratio in a logistic regression model predicting ACR, the next strongest independent predictor of ACR was the ratio of quinolate to X-16397, a metabolite of unknown identity. Analysis of the receiver operating characteristics (ROC) curve showed that the area under the curve (AUC) for 3SL/X was 0.75, and the signature at the Youden index¹⁵ based cut-off was diagnostic of ACR with a specificity of 76% and a sensitivity of 59% (Table 2). The ratio of quinolate to X-16397 also showed a strong association in the logistic regression model and a linear combination of the ratios of 3SL/X and quinolate to X-16397 increased the AUC from 0.75 to 0.81 and the Youden index from 36% to 53% (Table 2).

We examined whether any of the other metabolites and metabolite ratios reported

Table 1. Metabolite ratios and metabolite concentrations distinguishing ACR biopsies from No Rejection biopsies at a FDR of 5%

Metabolite Ratio or Metabolite	N ^a	beta ^b	P value ^c	P-gain ^c
3-Sialyllactose/Xanthosine	242	0.86	5.0×10 ⁻⁸	201,100
Neopterin/Xanthosine	234	0.90	2.0×10 ⁻⁸	72,220
3-(3-aminocarboxypropyl) Uridine/Xanthosine	242	0.83	1.6×10 ⁻⁷	61,644
3-Sialyllactose/X-16397 ^d	247	0.77	5.9×10 ⁻⁷	26,062
Quinolate/X-16397 ^d	248	0.89	7.3×10 ⁻⁹	25,031
Quinolate/4-hydroxymandelate	248	0.88	1.1×10 ⁻⁸	16,954
Neopterin/X-16570 ^d	235	0.84	9.7×10 ⁻⁸	14,493
Neopterin/N1-Methylguanosine	238	0.83	1.2×10 ⁻⁷	11,361
Proline	245	0.63	4.9×10 ⁻⁵	—
Quinolate	247	0.59	1.8×10 ⁻⁴	—
Isoleucine	244	0.58	2.1×10 ⁻⁴	—
X-13723 ^d	235	-0.57	3.7×10 ⁻⁴	—
X-12117 ^d	242	0.55	4.9×10 ⁻⁴	—
1,2,3 Benzenetriol sulfate	241	-0.55	5.8×10 ⁻⁴	—
Leucine	246	0.52	9.9×10 ⁻⁴	—
Pipecolate	239	0.52	1.1×10 ⁻³	—
Paraxanthine	158	-0.63	1.1×10 ⁻³	—
1,5-Anhydroglucitol	197	0.57	1.1×10 ⁻³	—
X-19434 ^d	126	0.77	1.3×10 ⁻³	—
Kynurenate	245	0.51	1.3×10 ⁻³	—
Neopterin	240	0.51	1.4×10 ⁻³	—
Myo-inositol	248	0.49	1.7×10 ⁻³	—
Gentisate	243	-0.50	1.8×10 ⁻³	—
Valine	243	0.49	1.9×10 ⁻³	—
N-Methyl-acetaminophen sulfate 1	175	0.58	2.5×10 ⁻³	—
Xylitol	248	-0.47	2.6×10 ⁻³	—

FDR, false discovery rate.

^aN is the number of urine samples with valid metabolite data following analysis of 248 urine samples from 185 patients matched to either ACR biopsies (number of urine samples=50; number of patients=36) or No Rejection biopsies (number of urine samples=198; number of patients=149). One No Rejection biopsy-associated sample contained insufficient material for metabolomics, and reduced the number of urine samples from 199 to 198, and the number of patients from 150 to 149, reported in the parent CTOT-04 study.¹ Urine samples matched to biopsies classified as borderline changes (number of urine samples=27; number of patients=25), AMR (number of urine samples=13; number of patients=11) or other biopsies (number of urine samples=9; number of patients=8) were also excluded from data analysis because the objective was to determine whether urine metabolite profiles distinguish ACR biopsies from No Rejection biopsies. The number of patients with a biopsy diagnosis exceeds the 190 patients providing 298 biopsy-matched urine samples because several patients had multiple biopsies with different biopsy diagnoses.

^bbeta is the slope of the linear model fitted to log₁₀-transformed and z-scored metabolite data (ion counts, coding of the independent variable: 0=No Rejection, 1=ACR).

^cP value and P-gain refer to the linear model metabolite or metabolite ratio=f (ACR); associations listed here are limited to those with a FDR of <5% for single metabolite associations. See Supplemental Table 3 for all nominally significant associations (i.e., with no adjustment for the number of tests) by linear regression and Supplemental Table 4 for all nominally significant associations by logistic regression. The top associations that emerged from these alternative statistical analyses were essentially the same, demonstrating the robustness of the association of metabolite profiles with ACR biopsy diagnosis.

^dAny metabolite of unknown structural identity is labeled as X-nnnnn (e.g., X-16397).

in Table 1 outperformed the combined metabolite signature of the ratios of 3SL/X and quinolate to X-16397, and none of the other metabolites or metabolite ratios did.

A Composite Metabolite and the mRNA Signature of ACR

We investigated the performance characteristics of the newly discovered metabolite signatures in combination with our previously established diagnostic signature of 18S rRNA and of 18S-normalized measures of CD3ε mRNA and IP-10 mRNA

in urinary cells. For consistency in the comparisons between the metabolite signatures and the mRNA signature we only used urine samples for which both metabolite and mRNA data were available for all computed signatures. Supplemental Tables 5 and 6 provide metabolite association data when samples without mRNA data were excluded.

To identify the combined metabolite- and mRNA-based signature, we performed a logistic regression analysis with $ACR=f(M_i, \text{mRNA signature})$, where M_i represents a log-scaled metabolite concentration or a log-scaled ratio between two metabolite concentrations. The log-scaled ratio of 3SL/X had the highest log-odds ratio (1.34, $P=1.6 \times 10^{-6}$) after inclusion of the mRNA signature in the model and thus represented the best candidate for a combined metabolite-mRNA signature (Supplemental Table 7). We selected the linear combination between log (3SL/X) and the mRNA signature that maximized the AUC. The resulting combined metabolite-mRNA signature was:

$$\text{mRNA-signature} + 1.1164 * \log(3SL/X).$$

Compared with the mRNA signature alone (AUC=0.84), the combined metabolite-mRNA signature had a significantly higher AUC of 0.91 (significance determined by random sampling, an AUC of 0.85 or below was observed in 95% of 1000 random samplings) (Table 2).

With the mRNA signature and the 3SL/X ratio included in the logistic analysis, the quinolate/X-16397 ratio was the next strongest predictor. With this additional metabolite ratio, the resulting combined signature that maximized the AUC was the following:

$$\text{mRNA-signature} + 1.1164 * \log(3SL/X) + 0.6937 * \log(\text{quinolate}/X-16397).$$

This combined two-metabolite-ratios-mRNA signature increased the AUC of the one-metabolite-ratio-mRNA signature to 0.93 (Table 2). This composite signature was diagnostic of ACR with a specificity of 84% and a sensitivity of 90%. Taken together, these results show that adding metabolite information to the mRNA signature substantially improves its diagnostic utility, as indicated by the > 30% increase in the Youden index

Table 2. Performance characteristics of the metabolite signature, mRNA diagnostic signature and the combined signature discriminating ACR biopsies from No Rejection biopsies

Signature ^{a,b}	AUC [95%]	Specificity (1-FP, %)	Sensitivity (TP, %)	Youden index, %
Log(3-sialyllactose/xanthosine)	0.75 [0.60]	76	59	36
Log(quinolinate/X-16397)	0.71 [0.60]	88	51	39
Log(3-sialyllactose/xanthosine) + 0.9513* log(quinolinate/ X-16397)	0.81 [0.77]	71	82	53
mRNA signature	0.84 [0.60]	72	85	56
mRNA signature+1.1164* log(3-sialyllactose/xanthosine)	0.91 [0.85]	82	87	69
mRNA signature + 0.8932* log(quinolinate/X-16397)	0.88 [0.85]	77	85	62
mRNA signature+1.1164* log(3-sialyllactose/xanthosine)+0.6937* log(quinolinate/X-16397)	0.93 [0.92]	84	90	74

^aThe signature that optimizes the AUC is given together [in square brackets] with the largest AUC that can be observed by chance ($P=0.05$) when the last term of the signature is randomized in the optimization procedure (95th percentile of 1000 randomizations). Sensitivity and specificity based on Youden index maximizing the difference between the true positive (TP) and the false positive (FP) rate for the signatures are listed.

^bTo make performance characteristics of the signatures comparable, the values shown in Table 2 were all computed using 198 urine samples from 154 patients (39 ACR biopsy urine samples from 31 patients and 159 No Rejection biopsy-matched urine samples from 123 patients) that contained both valid metabolite data and urinary cell mRNA signature score. This resulted in the mRNA signature having slightly different values in the metabolomics study compared with the values reported in the parent CTOT-04 study in which 43 ACR biopsy-matched urine samples from 34 patients and 163 No Rejection biopsy-matched urine samples from 126 patients were analyzed and the mRNA signature was diagnostic of ACR with a specificity of 78% and a sensitivity of 79% and the AUC by ROC curve analysis was 0.85.¹

from 56% for the mRNA signature alone to 74% for the combined two-metabolite-ratio-mRNA signature.

Among the 39 ACR biopsies from 31 patients (Table 2), 34 biopsies were for-cause biopsies and five biopsies were surveillance biopsies. Among the 159 No Rejection biopsies from 123 patients, 104 biopsies were for-cause biopsies and 55 biopsies were surveillance biopsies. The composite metabolite and mRNA signature distinguished the 34 for-cause ACR biopsies from the 104 for-cause No Rejection biopsies ($P=1.6 \times 10^{-17}$); the composite metabolite and mRNA signature distinguished also the five surveillance ACR biopsies from the 55 surveillance No Rejection biopsies ($P<0.001$).

Prognostic Performance of the Signatures

We examined whether the signatures, in addition to being diagnostic of ACR, predict future occurrence of an ACR. For this analysis, the day of kidney biopsy was designated as day 0 and a total of 337 urine samples with both urine metabolite data and urinary cell mRNA data and collected up to 1 year prior to an ACR biopsy or a No Rejection biopsy were analyzed to investigate whether the signatures predict future ACR biopsies. Data from this analysis are illustrated as bean plots (Figure 2). We chose this kind of data representation over box-and-whisker plots as it presents individual data points as one-dimensional scatter plots as well as representing the distribution of data points by the density shapes.¹⁶ The Youden cut-off of the respective signature for distinguishing ACR biopsies from No Rejection biopsies in biopsy-matched urine samples was used to calculate the sensitivity and the specificity of the signature at indicated time intervals and are included in Figure 2.

The ratio of 3SL/X in urine samples collected during 4 days to 30 days prior to biopsy predicted future development of an ACR with a specificity of 72% and a sensitivity of 59% (Figure 2A). The combination signature of ratios of 3SL/X and quinolinate to X-16397 in urine collected during the same time

interval predicted future ACR (Figure 2B), and the mRNA signature did not outperform either of the two-metabolite signatures (Figure 2C). A combination of the mRNA signature and the 3SL/X metabolite signature (Figure 2D) or a combination of the mRNA signature and the 3SL/X and quinolinate/X-16397 metabolite signatures in urine collected up to 30 days before a biopsy had the highest specificity but not the highest sensitivity for predicting future ACR (Figure 2E). It is important to note that the urine samples analyzed for their prognostic ability are pristine in the sense that they were not included in the initial step that led to the construction of the diagnostic metabolite or mRNA signatures and that these predictions are thus free of model bias.

Longitudinal Analysis in Clinically Stable Patients

A total of 385 sequential urine samples with both metabolite and mRNA data were analyzed to investigate the characteristics of the signatures in the first year of transplantation in clinically stable patients (legend to Figure 1 and Supplemental Material specify the criteria used to classify patients as clinically stable patients and the rationale for the selection of 40 clinically stable patients for the longitudinal analysis). Data from the analysis of sequential urine samples, visualized as bean plots, show that the signatures are remarkably stable when measured in urine samples collected 30 days after kidney transplantation (Figure 3). The signatures' ability to predict No Rejection biopsies (specificity) progressively increased over time for all signatures and a combination of the metabolite signatures and the mRNA signature performed best, with specificity reaching 90% in urine samples collected during post-transplant days 271–365. It is noteworthy that none of the urine samples included in this longitudinal analysis were included in the initial construction of the diagnostic metabolite or mRNA signatures, and that the predictions shown in Figure 3 are therefore also free of model bias.

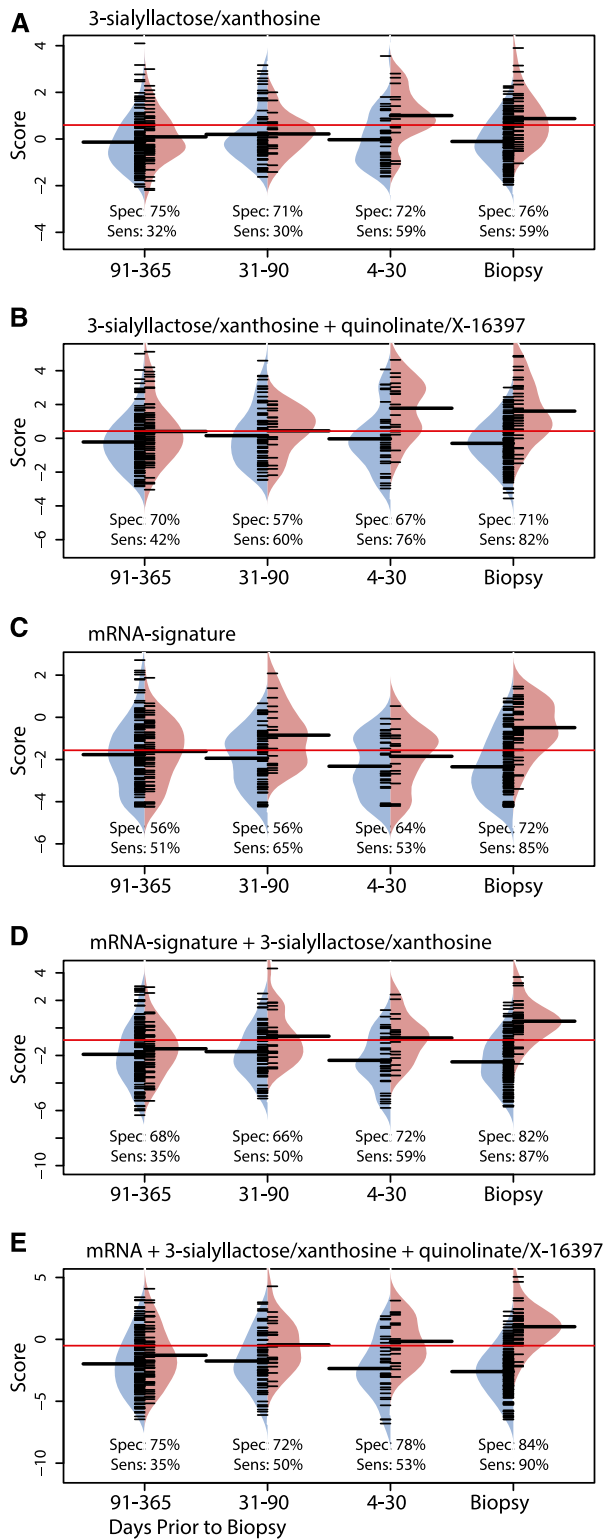


Figure 2. Bean plots, specificity, and sensitivity of signature scores in urine samples from patients with kidney allograft biopsies showing either ACR (light red) or No Rejection (normal, light blue). The day of kidney biopsy was designated as day 0 for all analyses and data from samples collected up to 365 days prior to biopsy are shown. Scores of metabolite signatures and the

Targeted Assay Development

For clinical application, we developed a high-throughput assay using robotic solid-phase (RapidFire 365) extraction and quadrupole time-of-flight–tandem mass spectrometry (MS/MS) for simultaneous absolute quantification of urinary 3-sialyllactose and xanthosine levels – metabolites suggested by our nontargeted metabolomics-to offer diagnostic and prognostic information regarding ACR. Notably, this novel platform allows for a theoretical urinary sample throughput of over 5000 samples daily. Because metabolite profiling results found that ACR diagnosis may be best afforded by considering the ratio of 3SL/X, rather than absolute metabolite levels, we optimized this platform for high-throughput ratiometric assay for these analytes (detailed in Supplemental Material and Supplemental Figure 1). To test the utility of this ratiometric approach, two or three repeated measurements of 3SL/X ratios were made for each of the 43 ACR biopsy-matched samples and 163 No Rejection biopsy-matched samples using a fresh, not previously thawed, aliquot of urine supernatant. The P value for the association of the ratio of 3SL/X for discriminating ACR biopsies from No Rejection biopsies was $P=4.0 \times 10^{-8}$ with the targeted RapidFire assay (Supplemental Figure 2), in accord with the P value obtained following analysis of nontargeted metabolomics data. The observed correlation between the nontargeted metabolon data and targeted RapidFire-quadrupole time-of-flight data was 0.65 (Pearson R) and the Bland–Altman method for

mRNA signature in 159 urine samples matched to 159 No Rejection biopsies and 39 samples matched to 39 ACR biopsies (biopsy-matched urine samples collected 3 days before to 1 day after the biopsy), 53 urine samples collected during 4 days to 30 days before the biopsy (36 samples from patients with future No Rejection biopsies and 17 from patients with future ACR biopsies), 88 urine samples collected during 31 days to 90 days before the biopsy (68 samples from patients with future No Rejection biopsies and 20 samples from patients with future ACR biopsies), and 196 urine samples collected during 91 days to 365 days before the biopsy (139 samples from patients with future No Rejection biopsies and 57 from patients with future ACR biopsies) are shown as thin black lines in the one-dimensional scatter plot. The distribution of signature scores are represented by the density shape, and the average for each distribution is shown as a thick black horizontal line crossing the contour of the individual bean plot. The red horizontal line across all bean plots indicates the Youden cut-off of the respective signature for distinguishing ACR biopsies from No Rejection biopsies in biopsy-matched urine samples. The Youden cut-off was used to calculate the sensitivity and the specificity of the signature for predicting ACR biopsies at the indicated time intervals. (A) Log ratio of 3SL/X, (B) a combination of log ratios of 3SL/X and quinolinate to X-16397, (C) the 18S rRNA-normalized measures of CD3 mRNA, IP-10 mRNA, and 18S rRNA signature (mRNA signature), (D) a combination of the log ratio 3SL/X and the mRNA signature, and (E) a combination of log ratios of 3SL/X and quinolinate to X-16397 and the mRNA signature. To present comparable datasets, urine samples with valid data for all five signatures in each of the time intervals analyzed were included to generate the bean plots.

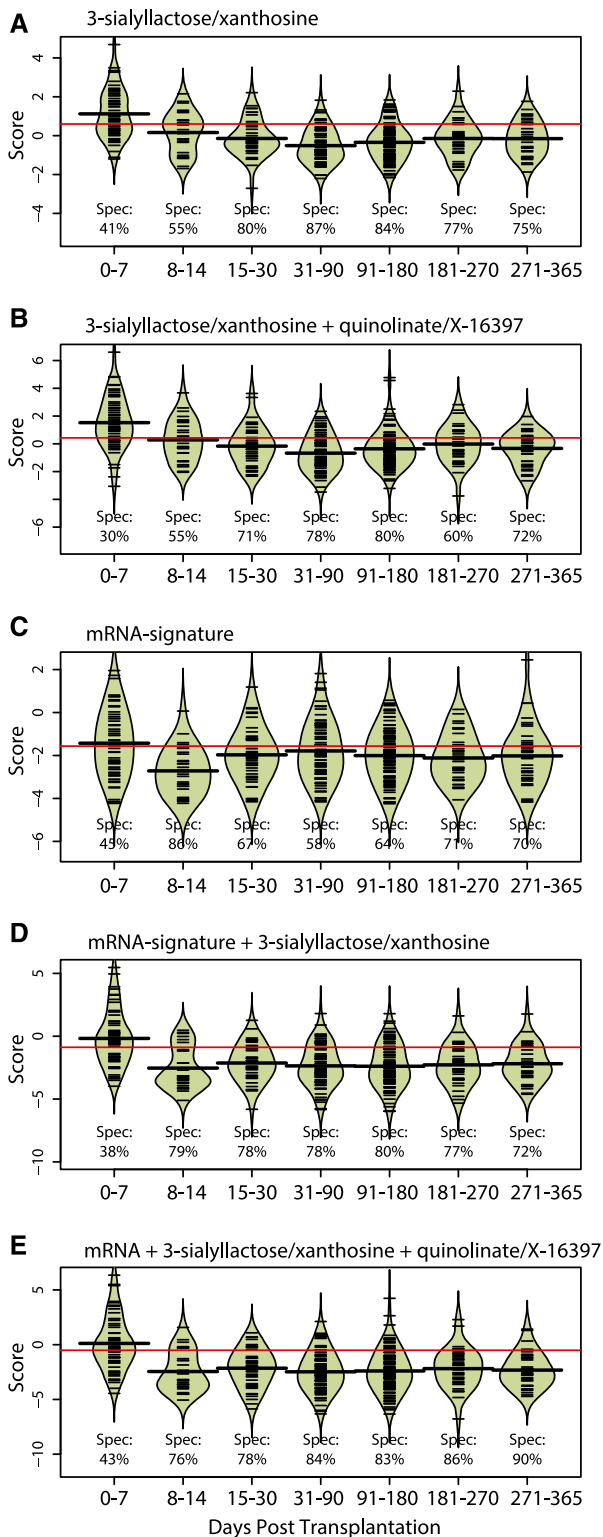


Figure 3. Bean plots and specificity of signature in sequential urine samples from 40 clinically stable patients. In the parent CTOT-04 study, sequential urine samples were collected on post-transplant days 3, 7, 15, and 30 and in months 2, 3, 4, 5, 6, 9, and 12. Criteria for classification as patients with stable graft function are listed in the legend to Figure 1. Scores of metabolite signatures and the mRNA

comparison¹⁷ showed that only 12 samples (6%) were beyond the 95% limit of agreement (Supplemental Figure 3). We could not develop a targeted assay for measuring the quinolinate/X-16397 ratio in view of the unknown structural identity of X-16397.

DISCUSSION

Promising results that metabolite profiles may serve as biomarkers of native kidney disease and of kidney allograft status have been reported.^{18–20} To our knowledge, the investigation summarized in this report is the largest prospective study of metabolite profiling of urine from kidney graft recipients, and also the first one to investigate the diagnostic accuracy of a composite signature of metabolites and mRNAs in urine.

We used a comprehensive combination of nontargeted liquid chromatography (LC)-MS/MS and gas chromatography (GC)-MS based metabolomics platforms to analyze 1516 urine samples from 241 kidney allograft recipients, and found metabolite signatures diagnostic of ACR. Moreover, the metabolite signature of the ratios of 3SL/X and quinolinate to X-16397 was complementary to the information contained in the mRNA signature, resulting in a composite metabolite–mRNA signature that was diagnostic of ACR with high accuracy. The composite metabolite and mRNA signature was diagnostic of ACR in patients who underwent for-cause biopsies and in patients who underwent surveillance biopsies. Applied to urine samples taken 4 to 30 days prior to biopsy, the signatures developed using only biopsy-matched urine samples predicted future ACR in pristine samples.

signature in the 56 urine samples collected during the first week of transplantation (0–7 days), 29 urine samples collected during week 2 post-transplant (8–14 days), 45 urine samples collected during post-transplant weeks 3 to 4 (15–30 days), 77 urine samples collected during post-transplant months 2 and 3 (31–90 days), 103 urine samples collected during months 4 to 6 post-transplant (91–180 days), 36 urine samples collected during months 7 and 9 post-transplant (181–270 days), and 40 urine samples collected during months 10 and 12 post-transplant (271–365 days) are shown as thin black lines in the one-dimensional scatter plot. The distribution of signature scores is represented by the density shape, and the average for each distribution is shown as a thick black horizontal line crossing the contour of the individual bean plot. The red horizontal line across all bean plots indicates the Youden cut-off of the respective signature for distinguishing ACR biopsies from No Rejection biopsies in biopsy-matched urine samples and the Youden cut-off was used to calculate specificity of the signatures. (A) Log ratio of 3SL/X, (B) a combination of log ratios of 3SL/X and quinolinate to X-16397, (C) the 18S rRNA-normalized measures of CD3 mRNA, IP-10 mRNA, and 18S rRNA signature (mRNA signature), (D) a combination of the log ratio 3SL/X and the mRNA signature, and (E) a combination of log ratios of 3SL/X and quinolinate to X-16397 and the mRNA signature.

Multivariate machine learning techniques and nonlinear fitting algorithms have been applied in biomarker searches. However, based on our experience analyzing data from metabolomics, and also to avoid the risk of over-fitting the data, we believe that metabolites showing a strong association in a linear univariate model are generally the most robust candidate clinical biomarkers.²¹ Also, the more metabolites that enter a metabolomics-based signature, the higher are the chances that one of the measurements may fail (*e.g.*, due to ion suppression in the presence of other metabolites) and thereby invalidate the entire signature. We therefore chose not to use more sophisticated biomarker discovery algorithms at this point.

Most essential for clinical application, we demonstrate that our metabolite marker, which was identified on a nontargeted metabolomics platform in a research setting, can be translated into a clinically applicable assay. This represents an important step toward the establishment of a clinically applicable, non-invasive biomarker of ACR, the most common type of acute rejection in kidney graft recipients. Our use of ratios of two urine metabolites (*e.g.*, 3SL/X) eliminates the problem of normalization and thus renders the biomarker more robust and easily applicable in the clinic. As we have previously noted²¹ and demonstrated here, ratios of metabolite concentrations can be developed efficiently into a targeted mass spectrometric assay as the ratio of two metabolite-specific fragmentation patterns, thereby obviating the need for measurement of an external calibration standard, such as urine creatinine or osmolality.

From a clinical perspective, our finding that the diagnostic signatures are remarkably stable in sequential urine samples collected from clinically stable patients raises the possibility that these signatures could help reduce the need for surveillance biopsies in this patient population. Our additional finding that the signatures cross the diagnostic threshold during the month prior to an ACR biopsy suggests that the signature could trigger a biopsy prior to changes in renal allograft function and help initiate pre-emptive anti-rejection therapy.

Our study, for the first time, links 3-sialyllactose to kidney allograft rejection. Proinflammatory (*e.g.*, stimulation of CD11c+ dendritic cells²²) as well as anti-inflammatory (*e.g.*, inhibition of cholera toxin²³) properties have been ascribed to this sialylated component that is also found in milk (HMDB00825). Also, sialyllactose may represent a molecular recognition pattern for dendritic cell capture²⁴ and contribute to alloantigen presentation and triggering of acute rejection. Changes in sialyllactose levels have been noted in cells grown under bioenergetic or oxidative stress (S. Gross, unpublished observations), and their increased levels during ACR may represent aberrant membrane glycolipid metabolism in immune and/or kidney parenchymal cells.

Quinolate is a product of tryptophan metabolism and is generated from kynurenine via a spontaneous, nonenzymatic reaction, and then oxidized by quinolate phosphoribosyltransferase to nicotinic acid ribonucleotide, nicotinic acid adenine dinucleotide and nicotinamide adenine dinucleotide

(NAD+).²⁵ Quinolate, by serving as a precursor for the biosynthesis of NAD+, may help meet the metabolic demands of activated immune cells contributing to ACR.

Xanthosine is a nucleoside derived from the purine base xanthine and ribose. Xanthine monophosphate is produced by inosine monophosphate dehydrogenase (IMPDH) and is obligatory for proliferation of T and B cells. IMPDH inhibition by mycophenolic acid is a key mechanism by which mycophenolic acid reduces the incidence of acute rejection.^{26,27} A potential mechanism for the lower level of xanthosine during ACR is inefficient inhibition of IMPDH leading to efficient conversion of IMP to guanosine and consequent lack of substrate for xanthine biosynthesis.

Each year 15,000 or more kidney transplants are performed in the United States alone, and with an estimated incidence of 0.4 biopsies/patient during the first year of transplantation, the charges for performing 7000 or so biopsies in kidney graft recipients during the first year of transplantation alone can be estimated to be \$21 million, based on the reported charge of \$3000 per biopsy.^{28,29} Our finding that noninvasive diagnosis of ACR is feasible by measurement of just four metabolites and three transcripts in urine (estimated cost of the assay: \$250–\$300) has the potential to reduce biopsy-associated costs. It should be emphasized however that our study focused on patients with biopsy-confirmed ACR and patients with biopsies without rejection changes, and did not systematically evaluate the diagnostic performance in patients with allograft dysfunction due to other causes such as AMR or BK virus nephropathy. Future studies, adequately powered to distinguish patients with commonly observed causes of graft dysfunction, should help delineate the clinical utility of the signatures developed in this study.

CONCISE METHODS

Urine Sample Collection

Four hundred and eighty-five patients with end stage renal disease were enrolled in the parent CTOT-04 multicenter, prospective observational study.¹ Five clinical sites enrolled the CTOT-04 study participants (additional information provided in Supplemental Material). Sequential urine samples were collected from the study participants on post-transplant days 3, 7, 15, and 30 and in months 2–6, 9, and 12 and at the time of biopsy. A total of 4300 urine samples were prospectively collected, and urine pellet and cell-free supernatants were prepared at each clinical site using a standard protocol. The urine cell pellets and the supernatants in aliquots were shipped to Weill Cornell Medical College Core Laboratory and stored at –80°C. Nontargeted metabolomics and targeted metabolite measurements were performed on aliquots of supernatants that were never thawed prior to metabolite analysis. Figure 1 and Supplemental Material provide information regarding sample selection for metabolite analysis. Supplemental Table 2 is a summary of the characteristics of the patients included in the analysis to develop the metabolite signatures and the composite metabolite and mRNA signature.

Metabolite Data Acquisition

Nontargeted metabolomics of urine was performed at Metabolon, Inc. (Durham, NC). Herein we report the essential steps that Metabolon performed on a fee-for-service basis for this study. Following receipt of samples by Metabolon, samples were inventoried and immediately stored at -80°C . At the time of analysis, samples were extracted and prepared for analysis using Metabolon's standard solvent extraction method. The extracted samples were split into equal parts for analysis on the GC/MS and LC/MS/MS platforms. Sample preparation was conducted using a proprietary series of organic and aqueous extractions to remove the protein fraction while allowing maximum recovery of small molecules. The resulting extract was divided into two fractions; one for analysis by LC and one for analysis by GC. The LC/MS portion of the platform was based on a Waters ACQUITY UPLC and a Thermo-Finnigan LTQ mass spectrometer, which consisted of an electrospray ionization source and linear ion trap mass analyzer. The GC/MS portion of the platform was analyzed on a Thermo-Finnigan Trace DSQ fast-scanning single-quadrupole mass spectrometer using electron impact ionization and operated at unit mass resolving power.

Metabolite Identification

The informatics system consisted of four major components, the Metabolon Laboratory Information Management System, the data extraction and peak identification software, data processing tools for QC and metabolite identification, and a collection of information interpretation and visualization tools for use by data analysts. Peaks were identified using Metabolon's proprietary peak integration software, and component parts were stored in a separate, specifically designed complex data structure. Metabolites were identified by comparison to library entries of purified standards or recurrent unknown entities. More than 3500 commercially available purified standard compounds have been acquired and registered into the Laboratory Information Management System for distribution to both the LC and GC platforms for determination of their analytical characteristics. Using the Metabolon platform, we obtained metabolite data (ion counts) for a total of 1516 urine samples. In total, 749 different metabolites from 65 metabolic pathways, including 368 metabolites of unknown identity, were identified on at least one of the three mass spectrometry-based metabolomics platforms (Supplemental Table 1). A first data normalization step was performed to correct for variation resulting from instrument inter-day tuning differences. Essentially, each compound was corrected in run-day blocks by registering the medians to equal one and normalizing each data point proportionately. Values were then divided by urine osmolality and \log_{10} -scaled. Outliers > 4 SDs from the mean were removed. Mean and SD values were determined on the 5%–95% range of the data for this purpose. It was rare that > 2 outlier values were removed from a metabolite. Finally, the data were z-scaled (mean=0, SD=1).

Statistical Analyses

R and R-studio (R-project, versions 2.12.1 and 3.0.1) and IBM SPSS (IBM, version 21) were used for statistical analysis. Linear models were computed using the *lm*-package, logistic models using the *glm*-package (family binomial), and ROC curves using the *ROC*-package. Linear regression [$M_i=f(\text{ACR status})$] and logistic regression [$\text{ACR}=f(M_i)$]

were computed for all 749 log-normalized and then z-scored metabolite data vectors (M_i) for all samples with valid data taken at the time of a biopsy diagnosed as either ACR (coded 1) or 'No Rejection' (coded 0). Full association data from these analyses are provided in Supplemental Tables 3 and 4. Similarly, linear and logistic regressions were also computed, limiting the sample set further to samples with both metabolite data and successful mRNA quantification, *i.e.*, samples with available mRNA signatures. Full association data from these analyses are provided in Supplemental Tables 5–7.

The level of significance for association of a metabolite after Bonferroni correction at a nominal level of significance of 0.05 is a $P < 6.7 \times 10^{-5}$ ($=0.05/749$). Previous studies suggest that testing all possible combinations of ratios between metabolite concentrations may reveal new and biologically relevant associations in an unbiased approach.³⁰ We therefore included all pairs of metabolite ratios in our association tests. For the ratios, the significance level after Bonferroni correction is $P < 1.8 \times 10^{-7}$ ($=0.05/(749 \times 748/2)$). Note that since our data are log-scaled, the symmetry $\log(a/b) = -\log(b/a)$ halves the multiple testing burden. A ratio between two metabolites of which one already shows a strong association signal may suggest false positive implication of the other in the association. We therefore also require the *P*-gain statistic to be significant after Bonferroni correction. The *P*-gain is defined as the change in the *P* values of the association of the two single metabolites when compared with their ratio. An association of a ratio is thus considered significant if *P*-gain > 7490 ($=10 \times 749$) and *P* value $< 1.8 \times 10^{-7}$. Due to the inherent correlations among metabolic traits, the less conservative false discovery rate, introduced by Benjamini-Hochberg¹³ is generally used in metabolomics studies. In order not to miss metabolites of potential biologic interest we report associations that are significant at the false discovery rate of 5% in Table 1, and all nominal associations in Supplemental Tables 3–7.

Study Approval

The collection of urine specimens and clinical information were approved by the institutional review board at each of the five clinical sites (Northwestern University Feinberg School of Medicine, New York Presbyterian Hospital-Weill Cornell Medical Center, Hospital of University of Pennsylvania, New York Presbyterian Hospital-Columbia University Medical Center, and University of Wisconsin Hospital and Clinics). All subjects provided written informed consent prior to participating in the CTOT-04 study. The authors declare that this study adhered to the Declaration of Helsinki and Declaration of Istanbul.

ACKNOWLEDGMENTS

This work was supported in part by Biomedical Research Program funds at Weill Cornell Medical College in Qatar, a program funded by the Qatar Foundation, U01-AI63589, R37-AI051652 and R37-HL087062 from the National Institutes of Health, and a Clinical and Translational Science Center award (UL1-RR024996) to Weill Cornell Medical College.

Dr. Thangamani Muthukumar is a recipient of a K08-DK087824 from the National Institutes of Diabetic and Digestive and Kidney Diseases and Dr. John Lee is a recipient of a KL2 Scholars Award from the Weill Cornell Clinical and Translational Science Center (KL2-TR000458 from the National Center for Advancing Translational Sciences).

We thank Ms. Catherine Snopkowski (Weill Cornell Medical College, New York, NY), Ms. Jane Charette (Northwestern University Feinberg School of Medicine, Chicago, IL), Ms. Debra McCorristan (University of Pennsylvania, Philadelphia, PA), Dr. Amy Sundberg (University of Wisconsin Hospitals and Clinics, Madison, WI), and Mr. Jonathan Kim (Columbia University College of Physicians and Surgeons, New York, NY) for their substantive contributions to the execution of the parent CTOT-04 study.

DISCLOSURES

E.D.K. and R.P.M. are employees of Metabolon, Inc., a commercial provider of metabolomics services. The other authors have declared that no conflict of interest exists.

REFERENCES

- Suthanthiran M, Schwartz JE, Ding R, Abecassis M, Dadhania D, Samstein B, Knechtle SJ, Friedewald J, Becker YT, Sharma VK, Williams NM, Chang CS, Hoang C, Muthukumar T, August P, Keslar KS, Fairchild RL, Hricik DE, Heeger PS, Han L, Liu J, Riggs M, Ikle DN, Bridges ND, Shaked A; Clinical Trials in Organ Transplantation 04 (CTOT-04) Study Investigators: Urinary-cell mRNA profile and acute cellular rejection in kidney allografts. *N Engl J Med* 369: 20–31, 2013
- Hricik DE, Nickerson P, Formica RN, Poggio ED, Rush D, Newell KA, Goebel J, Gibson IW, Fairchild RL, Riggs M, Spain K, Ikle D, Bridges ND, Heeger PS; CTOT-01 consortium: Multicenter validation of urinary CXCL9 as a risk-stratifying biomarker for kidney transplant injury. *Am J Transplant* 13: 2634–2644, 2013
- Bouatra S, Aziat F, Mandal R, Guo AC, Wilson MR, Knox C, Bjorndahl TC, Krishnamurthy R, Saleem F, Liu P, Dame ZT, Poelzer J, Huynh J, Yallou FS, Psychogios N, Dong E, Bogumil R, Roehring C, Wishart DS: The human urine metabolome. *PLoS ONE* 8: e73076, 2013
- Bohra R, Klepacki J, Klawitter J, Klawitter J, Thurman JM, Christians U: Proteomics and metabolomics in renal transplantation—quo vadis? *Transpl Int* 26: 225–241, 2013
- Psychogios N, Hau DD, Peng J, Guo AC, Mandal R, Bouatra S, Sinelnikov I, Krishnamurthy R, Eisner R, Gautam B, Young N, Xia J, Knox C, Dong E, Huang P, Hollander Z, Pedersen TL, Smith SR, Bamforth F, Greiner R, McManus B, Newman JW, Goodfriend T, Wishart DS: The human serum metabolome. *PLoS ONE* 6: e16957, 2011
- Nicholson JK, Lindon JC: Systems biology: Metabonomics. *Nature* 455: 1054–1056, 2008
- Fiehn O: Metabolomics—the link between genotypes and phenotypes. *Plant Mol Biol* 48: 155–171, 2002
- Pauling L, Robinson AB, Teranishi R, Cary P: Quantitative analysis of urine vapor and breath by gas-liquid partition chromatography. *Proc Natl Acad Sci U S A* 68: 2374–2376, 1971
- Suhre K, Shin SY, Petersen AK, Mohney RP, Meredith D, Wägele B, Altmaier E, CARDIoGRAMDeloukas P, Erdmann J, Grundberg E, Hammond CJ, de Angelis MH, Kastenmüller G, Köttgen A, Kronenberg F, Mangino M, Meisinger C, Meitinger T, Mewes HW, Milburn MV, Prehn C, Raffler J, Ried JS, Römisch-Margl W, Samani NJ, Small KS, Wichmann HE, Zhai G, Illig T, Spector TD, Adamski J, Soranzo N, Gieger C: Human metabolic individuality in biomedical and pharmaceutical research. *Nature* 477: 54–60, 2011
- Gall WE, Beebe K, Lawton KA, Adam KP, Mitchell MW, Nakhle PJ, Ryals JA, Millburn MV, Nannipieri M, Camastra S, Natali A, Ferrannini E; RISC Study Group: Alpha-hydroxybutyrate is an early biomarker of insulin resistance and glucose intolerance in a nondiabetic population. *PLoS ONE* 5: e10883, 2010
- Sreekumar A, Poisson LM, Rajendiran TM, Khan AP, Cao Q, Yu J, Laxman B, Mehra R, Lonigro RJ, Li Y, Nyati MK, Ahsan A, Kalyana-Sundaram S, Han B, Cao X, Byun J, Omenn GS, Ghosh D, Pennathur S, Alexander DC, Berger A, Shuster JR, Wei JT, Varambally S, Beecher C, Chinnaiyan AM: Metabolomic profiles delineate potential role for sarcosine in prostate cancer progression. *Nature* 457: 910–914, 2009
- Spratlin JL, Serkova NJ, Eckhardt SG: Clinical applications of metabolomics in oncology: a review. *Clin Cancer Res* 15: 431–440, 2009
- Benjamini Y, Hochberg Y: Controlling the false discovery rate: a practical and powerful approach to multiple testing. *J R Stat Soc Series B Methodol* 57: 289–300, 1995
- Petersen AK, Krumsiek J, Wägele B, Theis FJ, Wichmann HE, Gieger C, Suhre K: On the hypothesis-free testing of metabolite ratios in genome-wide and metabolome-wide association studies. *BMC Bioinformatics* 13: 120, 2012
- Le CT: A solution for the most basic optimization problem associated with an ROC curve. *Stat Methods Med Res* 15: 571–584, 2006
- Peter K: Beanplot: A boxplot alternative for visual comparison of distributions. *J Stat Softw* 28: 1–9, 2008
- Bland JM, Altman DG: Statistical methods for assessing agreement between two methods of clinical measurement. *Lancet* 1: 307–310, 1986
- Blydt-Hansen TD, Sharma A, Gibson IW, Mandal R, Wishart DS: Urinary metabolomics for noninvasive detection of borderline and acute T cell-mediated rejection in children after kidney transplantation. *Am J Transplant* 14: 2339–2349, 2014
- Goek ON, Prehn C, Sekula P, Römisch-Margl W, Döring A, Gieger C, Heier M, Koenig W, Wang-Sattler R, Illig T, Suhre K, Adamski J, Köttgen A, Meisinger C: Metabolites associate with kidney function decline and incident chronic kidney disease in the general population. *Nephrol Dial Transplant* 28: 2131–2138, 2013
- Goek ON, Döring A, Gieger C, Heier M, Koenig W, Prehn C, Römisch-Margl W, Wang-Sattler R, Illig T, Suhre K, Sekula P, Zhai G, Adamski J, Köttgen A, Meisinger C: Serum metabolite concentrations and decreased GFR in the general population. *Am J Kidney Dis* 60: 197–206, 2012
- Suhre K, Römisch-Margl W, de Angelis MH, Adamski J, Luippold G, Augustin R: Identification of a potential biomarker for FABP4 inhibition: the power of lipidomics in preclinical drug testing. *J Biomol Screen* 16: 467–475, 2011
- Kurakevich E, Hennet T, Hausmann M, Rogler G, Borsig L: Milk oligosaccharide sialyl(α 2,3)lactose activates intestinal CD11c+ cells through TLR4. *Proc Natl Acad Sci U S A* 110: 17444–17449, 2013
- Idota T, Kawakami H, Murakami Y, Sugawara M: Inhibition of cholera toxin by human milk fractions and sialyllactose. *Biosci Biotechnol Biochem* 59: 417–419, 1995
- Izquierdo-Useros N, Lorizate M, Contreras FX, Rodriguez-Plata MT, Glass B, Erkizia I, Prado JG, Casas J, Fabriàs G, Kräusslich HG, Martinez-Picado J: Sialyllactose in viral membrane gangliosides is a novel molecular recognition pattern for mature dendritic cell capture of HIV-1. *PLoS Biol* 10: e1001315, 2012
- Moffett JR, Namboodiri MA: Tryptophan and the immune response. *Immunol Cell Biol* 81: 247–265, 2003
- Hartono C, Muthukumar T, Suthanthiran M: Immunosuppressive drug therapy. *Cold Spring Harb Perspect Med* 3: a015487, 2013
- Sollinger HW; U.S. Renal Transplant Mycophenolate Mofetil Study Group: Mycophenolate mofetil for the prevention of acute rejection in primary cadaveric renal allograft recipients. *Transplantation* 60: 225–232, 1995

28. Collins AJ, Foley RN, Chavers B, Gilbertson D, Herzog C, Johansen K, Kasiske B, Kutner N, Liu J, St Peter W, Guo H, Gustafson S, Heubner B, Lamb K, Li S, Peng Y, Qiu Y, Roberts T, Skeans M, Snyder J, Solid C, Thompson B, Wang C, Weinhandl E, Zuan D, Arko C, Chen SC, Daniels F, Ebben J, Frazier E, Hanzlik C, Johnson R, Sheets D, Wang X, Forrest B, Constantini E, Everson S, Eggers P, Agodoa L: 'United States Renal Data System 2011 Annual Data Report: Atlas of chronic kidney disease & end-stage renal disease in the United States. *Am J Kidney Dis* 59[A7]: e1–e420, 2012
29. Collins AJ, Kasiske B, Herzog C, Chavers B, Foley R, Gilbertson D, Grimm R, Liu J, Louis T, Manning W, Matas A, McBean M, Murray A, St Peter W, Xue J, Fan Q, Guo H, Li S, Roberts T, Snyder J, Solid C, Wang C, Weinhandl E, Arko C, Chen SC, Dalleska F, Daniels F, Dunning S, Ebben J, Frazier E, Johnson R, Sheets D, Forrest B, Berrini D, Constantini E, Everson S, Frederick P, Eggers P, Agodoa L: Excerpts from the United States Renal Data System 2004 annual data report: atlas of end-stage renal disease in the United States. *Am J Kidney Dis* 45: [A5–7], S1–S280, 2005
30. Dehaven CD, Evans AM, Dai H, Lawton KA: Organization of GC/MS and LC/MS metabolomics data into chemical libraries. *J Cheminform* 2: 9, 2010

This article contains supplemental material online at <http://jasn.asnjournals.org/lookup/suppl/doi:10.1681/ASN.2015010107/-/DCSupplemental>.